Journal of Sol-Gel Science and Technology (2023) 108:28–34
https://doi.org/10.1007/s10971-023-06183-x

ORIGINAL PAPER: FUNCTIONAL COATINGS, THIN FILMS AND MEMBRANES (INCLUDING DEPOSITION TECHNIQUES)

Sol–gel deposition of Al-doped ZnO thin films: effect of additional zinc supply

Koji Abe[1] · Tasuku Kubota[1]

Received: 9 March 2023 / Accepted: 24 June 2023 / Published online: 8 July 2023

Abstract

Al-doped ZnO (AZO) films were deposited by sol–gel method. Precursor solutions for sol–gel method usually contain oxygen sources such as water, ethanol, and acetates. Zinc vacancy acceptors tend to be formed under oxygen-rich growth conditions. In this study, glass substrates with a zinc layer were used to supply zinc to the AZO films during calcination annealing. The diffraction peaks of wurtzite ZnO were observed in XRD patterns, and no diffraction peaks corresponding to zinc metal were observed. The AZO films were transparent in the visible range. The average transmittance (400–800 nm) was above 86%. The electrical properties of the AZO films were improved by using the substrates with a zinc layer. The AZO film deposited on the glass substrate with a 100-nm-thick zinc layer showed a resistivity of $9.4 \times 10^{-4}\,\Omega\,\mathrm{cm}$.

Graphical Abstract

(**a**) Typical samples before and after annealing. (**b**) Resistivity of the AZO films as a function of the zinc layer thickness on the glass substrates. The AZO film deposited on the glass substrate with a 100-nm-thick zinc layer had a resistivity of 9.4×10^4 Ωcm.

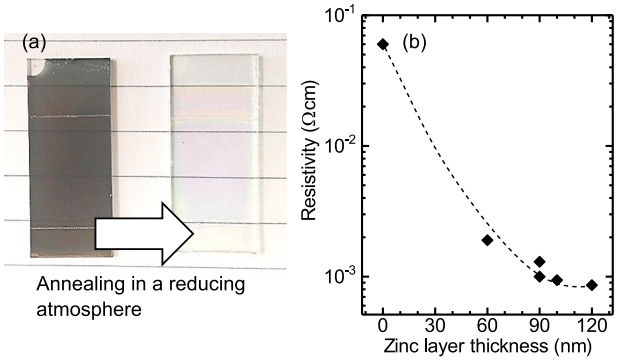

Keyword Zinc oxide · Transparent conductive oxide · Sol–gel · Dip-coating

Highlights

- Low-resistivity Al-doped ZnO (AZO) films were deposited by sol-gel method using glass substrates with a zinc layer.
- The AZO films after calcination annealing were transparent. The average transmittance (400–800 nm) of the AZO films was above 86%.
- The AZO film deposited on the glass substrate with a 100-nm-thick zinc layer had a resistivity of $9.4 \times 10^{-4}\,\Omega\,\mathrm{cm}$.

✉ Koji Abe
abe@nitech.ac.jp

[1] Department of Electrical and Mechanical Engineering, Nagoya Institute of Technology, Gokiso, Showa, Nagoya 466-8555, Japan

1 Introduction

Transparent conductive oxide (TCO) films are widely used in optoelectronic devices. Indium tin oxide (ITO) and zinc oxide (ZnO) are well-known TCO materials. ZnO is an earth-abundant and non-toxic semiconductor with a band gap energy of 3.37 eV. Impurities such as Al and Ga are effective shallow donors in ZnO, and low-resistivity ZnO thin films are deposited by various methods. Al-doped (AZO) and Ga-doped ZnO (GZO) films grown by chemical vapor deposition (CVD), sputtering, and pulsed laser deposition show a resistivity of the order of $10^{-4}\,\Omega\,\mathrm{cm}$ [1–4]. The ZnO films prepared by these vacuum deposition techniques have very good characteristics for TCO applications. Non-vacuum deposition techniques are also used for the synthesis of ZnO [5–7]. Spray pyrolysis and sol–gel method can be applied for ZnO thin film fabrication. Sol–gel dip-coating is known as a simple and cost-effective method. However, resistivity of sol–gel derived ZnO films is higher than that of vacuum-deposited ones [8–11]. Electrical properties of ZnO are known to be affected by intrinsic defects as well as donor and acceptor impurities. Necib et al. have studied the effects of film thickness on the properties of AZO films prepared by sol–gel method [12]. Winarski et al. have reported that ZnO films deposited by sol–gel method contain a high concentration of intrinsic defects [13]. Zinc vacancies in n-type ZnO are compensating acceptors, and oxygen vacancies are deep donors that cannot contribute n-type conductivity [14]. These intrinsic defects in ZnO are known to be passivated by annealing in an atmosphere containing hydrogen [13–15]. Zinc vacancy acceptors are passivated by hydrogen, and hydrogen bound in an oxygen vacancy acts as a shallow donor [16, 17]. However, it is difficult to reduce the zinc vacancy concentration in sol–gel derived ZnO films because the precursor solutions for sol–gel method usually contain oxygen sources such as water, ethanol, and acetates. Excessive oxygen is supplied from these oxygen sources. During calcination annealing, zinc vacancy acceptors tend to be formed under oxygen-rich growth conditions.

It is reported that annealing under zinc-rich conditions reduces the resistivity of sol–gel derived ZnO and $Mg_xZn_{1-x}O$ films [13, 18]. Yamada et al. have reported that ZnO films with a high electron concentration are obtained by annealing ZnO/Zn/ZnO sandwiched films [19]. They have also reported that annealing at temperatures above 400 °C desorbs zinc and reduce the electron concentration in ZnO films [20]. These papers indicate that zinc supply to suppress the formation of zinc vacancies is important to obtain low-resistivity ZnO films for TCO applications. As described above, however, ZnO deposition by sol–gel method is performed under oxygen-rich conditions. Additional zinc sources are required for the deposition of low-resistivity ZnO films by sol–gel method. Zinc salts contain ions such as Cl^- and NO_3^- that can affect properties of ZnO films. Zinc metal is not soluble in ethanol solution and cannot be added to the precursor solutions. In this study, we used glass substrates with a zinc layer as an additional zinc source. AZO films were deposited on the substrates by sol–gel method. The effects of the zinc layer thickness on the structural and electrical properties of AZO films will be described.

2 Experimental

Soda-lime glass substrates were cleaned with acetone, treated with a mixture of sulfuric acid and hydrogen peroxide, and rinsed in deionized water. After the cleaning, zinc layers were deposited on the substrates by radio frequency magnetron sputtering in pure argon at room temperature. The thickness of the zinc layer, which was controlled by the deposition time, was approximately 0, 60, 90, 100, and 120 nm. After the zinc layer deposition, the substrates were placed on a hotplate at 270 °C in air for 10 min to prevent the zinc layer from dissolving in the precursor solution. The precursor solution was prepared by adding zinc acetate dihydrate (1.65 g), aluminum nitrate nonahydrate (Al/Zn = 2.5 at.%), and monoethanolamine (0.6 ml) to ethanol (30 ml), and the mixture was stirred with a magnetic stirrer for 1 h at room temperature. The precursor solution was coated on the substrates by dip-coating. The substrates after dip-coating were then dried on a hotplate at 270 °C in air for 10 min and cooled to room temperature. After repeating the dip-coating and drying cycle seven times, the substrates were annealed in reducing atmosphere. Shirahata et al. have reported that when the growth temperatures are lower than 500 °C, low-resistive AZO films are not obtained by mist-CVD using zinc acetate as a zinc source [21]. Zhu et al. have reported that hydrogen addition during ZnO growth can deactivate deep levels in ZnO [22]. Thus, calcination annealing was carried out at 520 °C in a gas mixture of H_2 and Ar (H_2/Ar = 40%) for 1 h. After the calcination annealing, the substrates were re-annealed at 400 °C in H_2 for 20 min to improve the electrical properties of the AZO films. The obtained AZO films are denoted as zn-0, zn-60, zn-90, zn-100, and zn-120, depending on the zinc layer thickness on the substrates. Surface morphologies and structural properties of the AZO films were observed using scanning electron microscope (SEM, JEOL JSM-7800F) and X-ray diffraction (XRD, Rigaku SmartLab SE). Chemical composition was estimated by energy dispersive X-ray spectroscopy (EDS, Oxford Instruments) analysis, and the depth profile of elements in the AZO films was measured by Auger electron spectroscopy (AES, JAMP-9500F). Hall effect

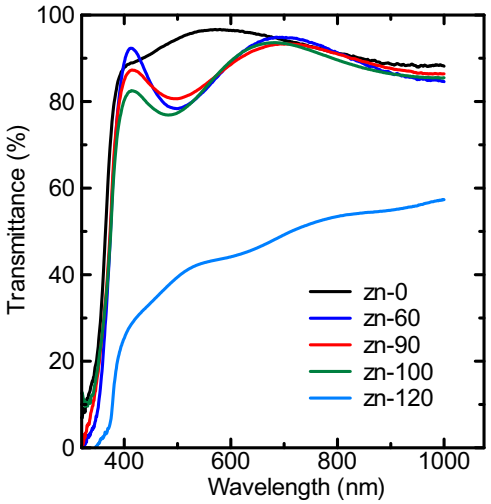

Fig. 1 Optical transmittance spectra of the AZO films deposited on the substrates with a different zinc layer thickness

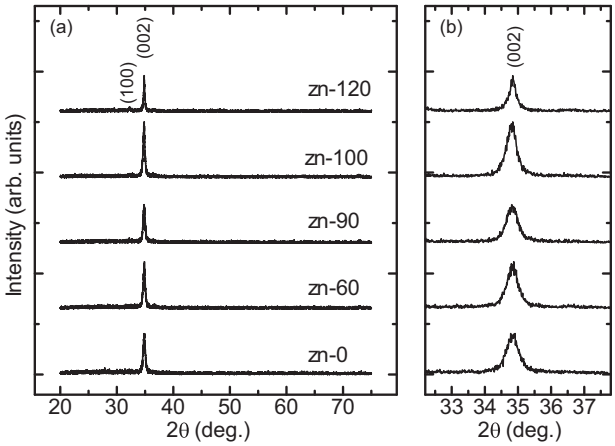

Fig. 2 **a** XRD patterns of the AZO films deposited on the substrates with a different zinc layer thickness. **b** Enlarged view of the XRD patterns

measurements were performed by using van der Pauw configuration.

3 Results and discussion

The samples before annealing were opaque due to the zinc layer on the substrate. As the zinc layer was consumed during the calcination annealing in an Ar/H_2 gas mixture, the AZO films except for the sample zn-120 showed high optical transmittance in the visible range. Figure 1 shows the optical transmittance spectra of the AZO films deposited on the substrates with a different zinc layer thickness. The transmittance for zn-60 and zn-90 was as high as that for zn-0. The average transmittance of zn-60, zn-90, and zn-100 (400–800 nm) was above 86%. The zinc layer below 90 nm had no significant influence on the optical transmittance spectra. However, when the zinc layer thickness increased to 100 nm, the optical transmittance between 400 and 500 nm slightly decreased due to the zinc supply from the zinc layer. Annealing in the presence of zinc vapor is reported to change the color of ZnO from transparent to red [23, 24]. In contrast, the sample zn-120 showed very low optical transmittance. The excessive zinc supply from the 120-nm-thick zinc layer resulted in the very low optical transmittance.

The XRD patterns for the AZO films deposited on the substrates with a different zinc layer thickness are shown in Fig. 2. The diffraction peaks of wurtzite ZnO were observed in the XRD patterns, and no diffraction peaks corresponding to zinc metal were observed. The samples had a c-axis preferential orientation. The 2θ value of the ZnO (002) diffraction peak was about 34.8°. It was larger than the standard diffraction data of wurtzite ZnO (JCPDS 36-1451). However, X-ray diffraction peaks are known to differ depending on the deposition conditions. The ZnO (002) diffraction peak at around 34.8° has also been reported by other groups [11, 25, 26]. The 2θ value did not depend on the zinc layer thickness. The full width at half maximum (FWHM) of the ZnO (002) diffraction peak for the samples zn-0, zn-60, zn-90, zn-100, and zn-120 was 0.48°, 0.38°, 0.41°, 0.37°, and 0.26°, respectively. The FWHM value was decreased by using the substrates with a zinc layer. The decrease in FWHM value indicates that zinc supply from the zinc layer improves the crystallinity of the AZO films. The sample zn-120 had a minimum FWHM value, but the ZnO (100) diffraction peak was observed in the XRD pattern. The excessive zinc supply from the 120-nm-thick zinc layer degraded the crystallinity.

Figure 3 shows the surface and cross-sectional SEM images and EDS spectra of the AZO films. A granular structure with round-shaped particles was observed on the surface of the sample zn-0. The AZO film deposited on the substrate without a zinc layer may consist of such particles. As can be seen in Fig. 3d, the thickness of zn-0 was ~200 nm. The zinc layer on the substrates changed the morphology and thickness of the AZO films. Round-shaped particles were not observed on the surface of zn-90 and zn-120. The thickness of zn-90 was ~250 nm (Fig. 3e), which was almost same as that of zn-60 and zn-100 (not shown). The thickness of the AZO films was increased by using the substrates with a zinc layer. The calcination annealing was performed at 520 °C in a gas mixture of H_2 and Ar. The annealing temperature is above the melting point of zinc metal and enough for zinc atoms to diffuse in ZnO [20]. The increase in film thickness indicates that additional ZnO is grown from the zinc layer and the oxygen sources in the precursor solution. Particles with a size of about 100 nm were observed on the surface of zn-90, but the surface was

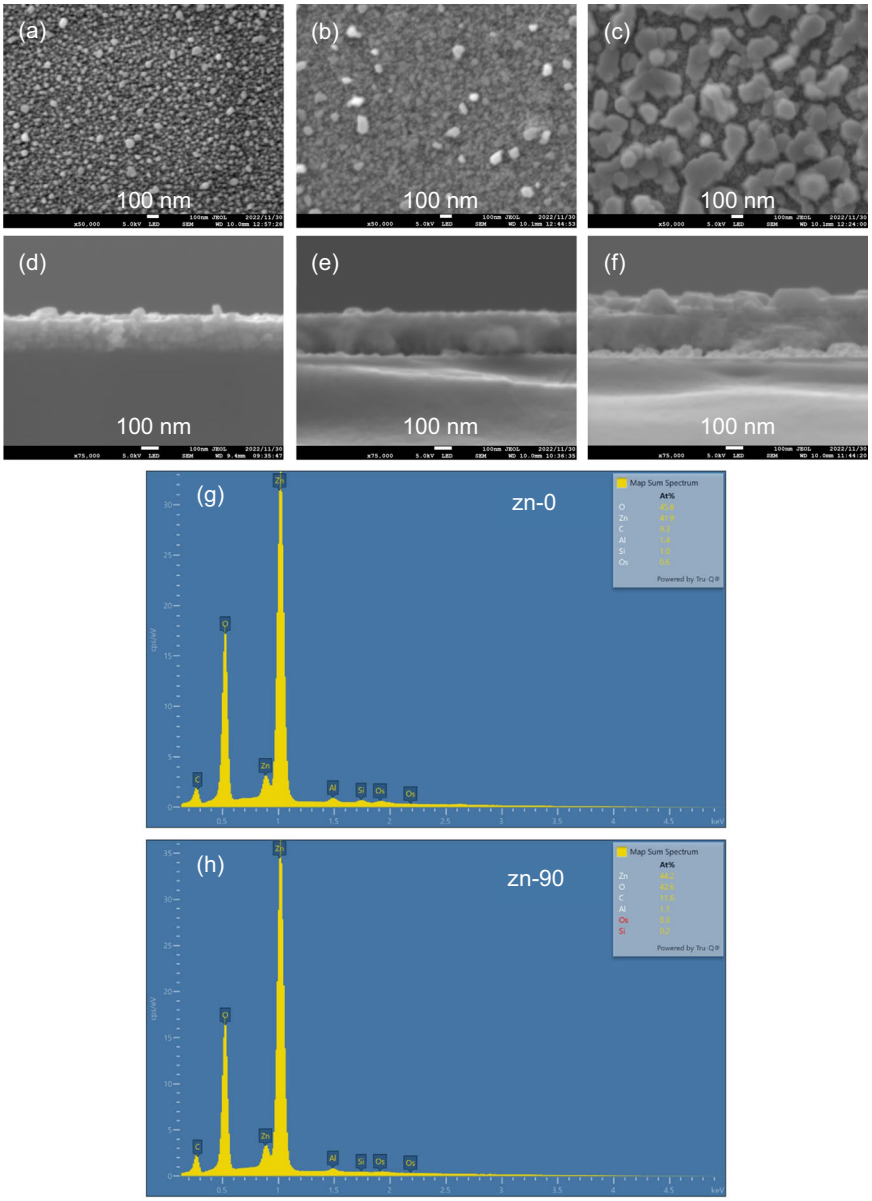

Fig. 3 **a**–**c** Surface SEM images, **d**–**f** cross-sectional SEM images, and **g**, **h** EDS spectra of the AZO films: **a**, **d** zn-0, **b**, **e** zn-90, **c**, **f** zn-120, **g** EDS spectrum for zn-0, and **h** EDS spectrum for zn-90

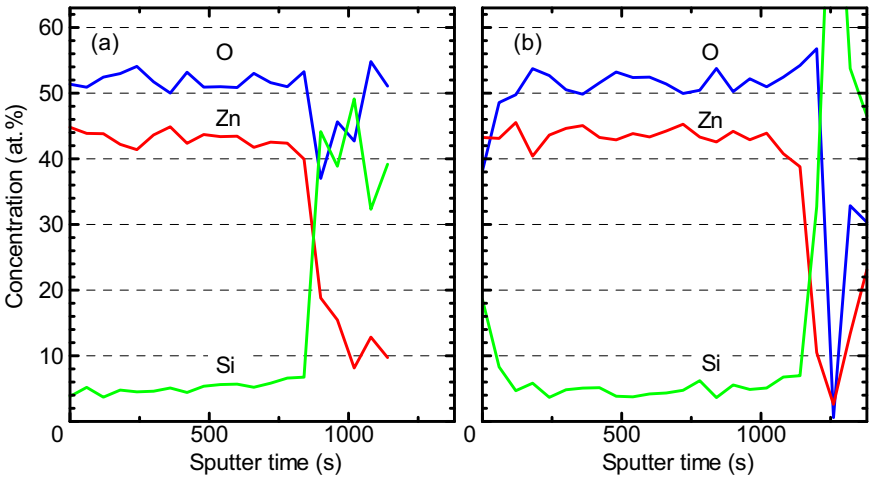

Fig. 4 Depth profiles of Zn, O, and Si in the AZO films: **a** zn-0 and **b** zn-90

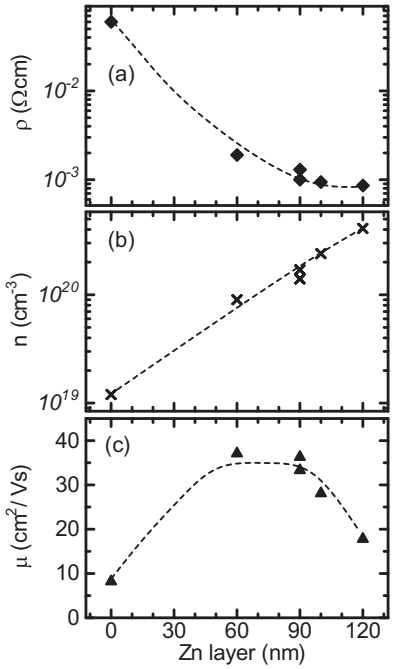

Fig. 5 Resistivity (ρ), carrier concentration (n), and Hall mobility (μ) of the AZO films deposited on the substrates with a different zinc layer thickness: **a** resistivity, **b** carrier concentration, and **c** Hall mobility. The dashed line in each graph is guide of eyes

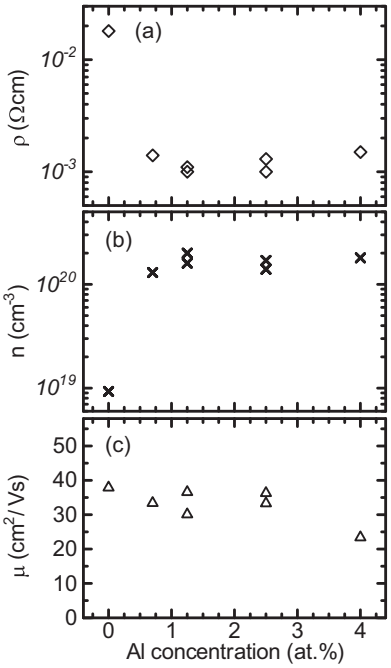

Fig. 6 Resistivity (ρ), carrier concentration (n), and Hall mobility (μ) of the AZO films as a function of the Al concentration in the precursor solution: **a** resistivity, **b** carrier concentration, and **c** Hall mobility. These AZO films were deposited on the substrates with a 90-nm-thick zinc layer

relatively smooth. On the other hand, large ZnO islands with a thickness of approximately 100 nm were observed on the surface of zn-120.

The chemical composition of the AZO films was estimated by EDS analysis. The EDS spectra for zn-0 and zn-90 were shown in Fig. 3g, h, respectively. Zn, O, Al, C, Si, and Os signals were detected. The Os signal was detected because of the osmium coating for the SEM observation. The C signal is originated from organic compounds in the precursor solution and/or surface contamination. The Si signal could be originated from the glass substrates. Figure 4 shows the depth profiles of Zn, O, and Si in the AZO films (zn-0 and zn-90). The depth profiles were measured by AES analysis. The Zn and O depth profiles in the AZO films were constant, indicating that the zinc layer was consumed by the additional ZnO growth and zinc desorption during the calcination annealing. This result is consistent with the XRD patterns in Fig. 2.

Figure 5 shows the resistivity, carrier concentration, and Hall mobility of the AZO films deposited on the substrates with a different zinc layer thickness. The dashed line in each graph is guide of eyes. The resistivity decreased and the carrier concentration increased with increasing zinc layer thickness. As shown in Fig. 1, these samples except for zn-120 were transparent in the visible range. The resistivity of zn-90 and zn-100 was $(1.0–1.3) \times 10^{-3}$ and $9.4 \times 10^{-4}\,\Omega\,\mathrm{cm}$, respectively. It is noteworthy that highly transparent and low-resistivity AZO films are obtained by sol–gel method. The Hall mobility was also increased by using the substrates with a zinc layer. The Hall mobility of zn-60, zn-90, and zn-100 was comparable to that of sputter-deposited ZnO films [2, 19, 27] but lower than that of high crystallinity ZnO films reported by Nomoto et al. [28]. The improved electrical properties can be due to the additional ZnO growth during the calcination annealing. Although the carrier concentration of zn-60 was lower than that of zn-90, the Hall mobility of zn-60 was almost same as that of zn-90 despite the lower carrier concentration. However, when the zinc layer thickness was between 90 and 120 nm, the Hall mobility decreased along with the increase in carrier concentration. The thickness of the zinc layer affects the additional ZnO growth during the calcination annealing. These results suggest that the zinc supply from the 60-nm-thick zinc layer was insufficient. The sample zn-120 showed low optical transmittance (Fig. 1). The electrical properties of zn-120 could have been affected by the excessive zinc supply.

AZO films with a different Al concentration were fabricated to investigate the effect of impurity doping. These AZO films were deposited on the substrates with a 90-nm-thick zinc layer. The resistivity, carrier concentration, and Hall mobility of the AZO films as a function of the Al concentration in the precursor solution are shown in Fig. 6. The Al concentration in the precursor solution was varied from 0 to 4 at.% (Al/Zn = 0, 0.7, 1.25, 2.5, and 4 at.%) by

changing the amount of aluminum nitrate nonahydrate. The carrier concentration of the ZnO film (Al/Zn = 0) was $9.3 \times 10^{18}\,cm^{-3}$, indicating that the background carrier concentration of the AZO films was about $10^{19}\,cm^{-3}$. The carrier concentration was increased by the Al doping. However, when the Al concentration was between 1.25 and 4 at.%, the carrier concentration showed no significant dependence on the Al concentration. Similar dependence of carrier concentration on Al doping has been reported by other groups [11, 29]. When the Al concentration was 4 at.%, the resistivity increased to $1.5 \times 10^{-3}\,\Omega\,cm$ due to the decrease in Hall mobility. The solubility limit of Al in wurtzite ZnO is reported to be lower than 3 at.% [30, 31]. The decrease in Hall mobility at the Al concentration of 4 at.% can be attributed to the solubility limit of Al. The optimum Al concentration in the precursor solution was between 1.25 and 2.5 at.%.

4 Conclusions

Low-resistivity AZO films were deposited by sol–gel method using glass substrates with a zinc layer. The zinc layer supplied zinc to the AZO films during the calcination annealing in a gas mixture of H_2 and Ar. Except for the sample deposited on the substrate with a 120-nm-thick zinc layer, the AZO films showed high optical transmittance in the visible range. The average transmittance of the AZO films (400–800 nm) was above 86%. However, the excessive zinc supply from the 120-nm-thick zinc layer resulted in the very low optical transmittance. The diffraction peaks of wurtzite ZnO were observed in the XRD patterns, and no diffraction peaks corresponding to zinc metal were observed. Since additional ZnO was grown from the zinc layer and the oxygen sources in the precursor solution, the thickness of the AZO films was increased by using the substrates with a zinc layer. The zinc layer was consumed during the calcination annealing, and the Zn and O depth profiles in the AZO films were constant. The electrical properties of the AZO films were improved by using the substrates with a zinc layer. The resistivity decreased and the carrier concentration increased with increasing zinc layer thickness. The improved electrical properties can be due to the additional ZnO growth during the calcination annealing. The AZO film deposited on the glass substrate with a 100-nm-thick zinc layer showed a resistivity of $9.4 \times 10^{-4}\,\Omega\,cm$. The optimum Al concentration (Al/Zn) in the precursor solution was between 1.25 and 2.5 at.%. The substrates with a zinc layer are very effective for the deposition of low-resistivity AZO films by sol–gel method.

Acknowledgements The authors would like to thank Ms. Noriko Asaka for her kind support for the SEM and EDS observations.

Author contributions All authors contributed to the study conception and design. Sample preparation, data collection, and analysis were performed by KA and TK. The first draft of the manuscript was written by KA, and all authors commented on previous versions of the manuscript. All authors read and approved the final manuscript.

Compliance with ethical standards

Conflict of interest The authors declare no competing interests.

References

1. Lu JG, Kawaharamura T, Nishinaka H, Kamada Y, Ohshima T, Fujita S (2007) ZnO-based thin films synthesized by atmospheric pressure mist chemical vapor deposition. J Cryst Growth 299:1–10
2. Minami T (2005) Transparent conducting oxide semiconductors for transparent electrodes. Semicond Sci Technol 20:S35–S44
3. Mickan M, Helmersson U, Horwat D (2018) Effect of substrate temperature on the deposition of Al-Doped ZnO thin films using high power impulse magnetron sputtering. Surf Coat Technol 347:245–251
4. Nian Q, Look D, Leedy K, Cheng GJ (2018) Optoelectronic performance enhancement in pulsed laser deposited gallium-doped zinc oxide (GZO) films after UV laser crystallization. Appl Phys A 124. https://doi.org/10.1007/s00339-018-2032-4
5. Perfetti C, Abe K (2017) Solution growth of zinc oxide on aluminum zinc layered double hydroxides. J Cryst Growth 468:650–654
6. Tang C, Chena K, Chen C (2018) Solution-processed ZnO/Si based heterostructures with enhanced photocatalytic performance. N J Chem 42:13797–13802
7. Sakai D, Nagashima K, Yoshida H, Kanai M, He Y, Zhang G, Zhao X, Takahashi T, Yasui T, Hosomi T, Uchida Y, Takeda S, Baba Y, Yanagida T (2019) Substantial narrowing on the Width of "concentration window" of hydrothermal ZnO nanowires via ammonia addition. Sci Rep 9:14160
8. Zhu MW, Ma HB, Jin PH, Jin YN, Jia N, Chen H, Liu CZ (2020) An insight into the low doping efficiency of Al in sol–gel-derived ZnO:Al films: role of the dopant chemical state. Appl Phys A 126. https://doi.org/10.1007/s00339-020-03670-8
9. Chen S, Warwick MEA, Binions R (2015) Effects of film thickness and thermal treatment on the structural and opto-electronic properties of Ga-doped ZnO films deposited by sol–gel method. Sol Energy Mater Sol Cells 137:202–209
10. Heitmann U, Westraadt J, O'Connell J, Jakob L, Dimroth F, Bartsch J, Janz S, Neethling J (2022) Spray pyrolysis of ZnO:In: characterization of growth mechanism and interface analysis on p-type GaAs and n-type Si Semiconductor Materials. ACS Appl Mater Interfaces 14:41149–41155
11. Schellens K, Capon B, De Dobbelaere C, Detavernier C, Hardy A, Van Bael MK (2012) Solution derived ZnO:Al films with low resistivity. Thin Solid Films 524:81–85
12. Necib K, Touam T, Chelouche A, Ouarez L, Djouadi D, Boudine B (2018) Investigation of the effects of thickness on physical properties of AZO sol-gel films for photonic device applications. J Alloy Compd. https://doi.org/10.1016/j.jallcom.2017.11.36
13. Winarski DJ, Anwand W, Wagner A, Saadatkia P, Selim FA, Allen M, Wenner B, Leedy K, Allen J, Tetlak S, Look DC (2016) Induced conductivity in sol-gel ZnO films by passivation or elimination of Zn vacancies. AIP Adv 6:095004
14. McCluskey MD, Jokela SJ (2009) Defects in ZnO. J Appl Phys 106:071101

15. Janotti A, Van de Walle CG (2007) Hydrogen multicentre bonds. Nat Mater 6:44–47
16. Lavrov EV, Weber J, Börrnert F, Van de Walle CG, Helbig R (2002) Hydrogen-related defects in ZnO studied by infrared absorption spectroscopy. Phys Rev B 66. https://doi.org/10.1103/PhysRevB.66.165205
17. Lavrov EV, Herklotz F, Weber J (2009) Identification of two hydrogen donors in ZnO. Phys Rev B, 79. https://doi.org/10.1103/PhysRevB.79.165210
18. Abe K, Morimoto Y (2021) The effects of the post-annealing with a Zn cap on the structural and electrical properties of sol-gel derived $Mg_xZn_{1-x}O$ films. Mater Res Express 8:025907
19. Yamada Y, Sancakoglu O, Sugiura R, Shoriki M, Funaki S (2020) Electrical resistivity reduction and spatial homogenization of Ga-doped ZnO film Zn layer insertion. Thin Solid Films 707:138069
20. Yamada Y, Inoue S, Kikuchi H, Funaki S (2018) Resistivity reduction in Ga-doped ZnO films with a barrier layer that prevents Zn desorption. Thin Solid Films 657:50–54
21. Shirahata T, Kawaharamura T, Fujita S, Orita H (2015) Transparent conductive zinc-oxide-based films grown at low temperature by mist chemical vapor deposition. Thin Solid Films 597:30–38
22. Zhu G, Gu S, Zhu S, Huang S, Gu R, Ye J, Zheng Y (2012) Optimization study of metal-organic chemical vapor deposition of ZnO on sapphire substrate. J Cryst Growth 349:6–11
23. Selim FA, Weber MH, Solodovnikov D, Lynn KG (2007) Nature of native defects in ZnO. Phys Rev Lett 99:085502
24. Weber MH, Lynn KG (2011) Hydrogen in red ZnO – defects or lattice expansion. J Phys Conf Ser 262:012063
25. Yang P, Wang J, Tsai W, Wang S, Lin J, Lee I, Chang C, Cheng H (2010) Photoresponse of hydrothermally grown lateral ZnO nanowires. Thin Solid Films 518:7328–7332
26. Santra S, Guha PK, Ali SZ, Hiralal P, Unalan HE, Covington JA, Amaratunga GAJ, Milne WI, Gardner JW, Udrea F (2010) ZnO nanowires grown on SOI CMOS substrate for ethanol sensing. Sens Actuators B: Chem 146:559–565
27. Novák P (2019) Possibilities of increasing the usability of sputtered AZO films as a transparent electrode. Phys Status Solidi A 216:1800814
28. Nomoto J, Makino H, Yamamoto T (2016) High-hall-mobility Al-doped ZnO films having textured polycrystalline structure with a well-defined (0001) orientation. Nanoscale Res Lett 11:320
29. Hou Q, Meng F, Sun J (2013) Electrical and optical properties of Al-doped ZnO and $ZnAl_2O_4$ films prepared by atomic layer deposition. Nanoscale Res Lett 8:144
30. Yoshioka S, Oba F, Huang R, Tanaka I, Mizoguchi T, Yamamoto T (2008) Atomic structures of supersaturated ZnO–Al_2O_3 solid solutions. J Appl Phys 103:014309
31. Yoon MH, Lee SH, Park HL, Kim HK, Jang MS (2002) Solid solubility limits of Ga and Al in ZnO. J Mater Sci Lett 21:1703–1704